ORIGINAL PAPER

CrossMark

Spatial variability analysis and mapping of soil physical and chemical attributes in a salt-affected soil

Masoomeh Delbari [1] (iD) · Peyman Afrasiab [1] · Bahram Gharabaghi [2] · Meysam Amiri [3] · Armand Salehian [1]

Abstract
Knowledge of inherent spatial variability of soil physical and chemical properties is needed for more accurate site-specific management of soil nutrients. In this study we investigated the spatial variability of a wide range of soil physical and chemical properties including soil texture fractions (percentages of sand, silt, and clay denoted as Sand, Silt and Clay, respectively), soil water content (WC), bulk density (BD), gypsum, organic carbon (OC), electrical conductivity (EC), pH, Ca, Mg, Na, *exchangeable* sodium percentage (ESP), sodium absorption ratio (SAR), available phosphorous (AP), and available potassium (AK) in a saline-alkaline soil catena in Sistan Plain, southeast of Iran. Soil samples were collected from two depths (0–15 and 15–30 cm) on a nearly regular grid at 113 sites over an 85-ha agricultural field. Statistical analysis of soil properties showed that Na, Mg, Ca, WC, EC, ESP, and SAR have a large coefficient of variation (CV) (more than 50%) and BD and pH have a low CV (less than 15%) for both layers. The correlation among soil properties varies for two layers; while Silt, WC, EC, ESP, Na, and gypsum are statistically ($p < 0.01$ and $p < 0.05$) correlated with most of physical and chemical properties in topsoil, Sand, EC, and OC are the most dominant properties in subsoil. Geostatistical autocorrelation analysis of soil properties were examined based on the "range of spatial continuity" and "nugget to sill" ratio. Accordingly, AP and subsoil ESP have the lowest spatial correlation while texture fractions are the most auto-correlated variables in space. The spatial structure of soil properties followed either a spherical or an exponential model with a minimum correlation distance of 70 m for AP to almost 800 m for soil fractions. The results indicated that spatial continuity generally increases and decreases with depth for soil physical and chemical properties, respectively. The difference in spatial variability of soil properties could be attributed to internal factors (e.g., the forming processes of soil) as well as external factors (e.g., human activities). The maps of soil physical and quality parameters were generated using either kriging or inverse distance weighting methods depending on cross-validation results. In general, topsoil layer has a greater amount of EC, ESP, SAR, pH, Na, Ca, Mg, and OC than subsoil while Silt, WC, and gypsum were often higher in subsoil. OC maps showed that the whole area is relatively low in organic carbon, mainly due to hot and dry climate and windy conditions in Sistan. The maps of soil nutrients provide useful information for adapting an efficient and precision agricultural production management.

Keywords Kriging · Spatial correlation · Soil nutrients · Site-specific management · Saline-sodic soil

✉ Masoomeh Delbari
  masoomeh.delbari@uoz.ac.ir

Peyman Afrasiab
  peyman.afrasiab@uoz.ac.ir

Bahram Gharabaghi
  bgharaba@uoguelph.ca

Meysam Amiri
  Meysam.Amiri@uoz.ac.ir

Armand Salehian
  armand.salehian@uoz.ac.ir

[1] Department of Water Engineering, Faculty of Water and Soil, University of Zabol, Zabol, Iran

[2] School of Engineering, University of Guelph, Guelph, ON, Canada

[3] Department of Water Resources, Hamoun International Wetland Research Institute, University of Zabol, Zabol, Iran

Springer

Introduction

Knowledge of spatial variability of soil physical and chemical properties helps to better understand the complicated relationship between soil and the environment (Goovaerts 1998; Afrasiab and Delbari 2013) and to determine an appropriate soil use management practice (Bouma et al. 1999; Safadoust et al. 2016a) such as variable rate application of soil nutrients (Geypens et al. 1999). It also allows for establishing an optimum sampling strategy (Blumfield et al. 2007; Brus and Heuvelink 2007; Wang et al. 2008), which may reduce sampling costs. Moreover several environmental models are getting popular for modeling many processes such as soil erosion and runoff (Morgan 2005; Stang et al. 2016), crop production (Basso et al. 2007; Basso and Ritchie 2015), and leaching of pollutants (Vachaud and Chen 2002; Safadoust et al. 2016b) in recent years. In order to minimize error propagation through these models, they must be based on an accurate characterization of the spatial variability of the soil properties used as input parameters (Goovaerts 1999). Knowledge of spatial variability of soil quality parameters such as soil organic carbon (SOC), soil texture, electrical conductivity (EC), and pH is essential for risk assessment and decision-making, e.g., giving correct site-specific recommendations or identifying the areas prone to degradation especially when agricultural productivity and environmental quality have to be sustained for future generations (Reeves 1997). Soil degradation decreases soil ecosystem services and agronomic production, and lessens economic growth, especially in countries where agriculture plays an important role in economic development (Lal 2015). Knowing the concentration of soil chemicals can be very important in presenting strategic plans for soil quality improvement and fertilizer management (Schepers et al. 2000). For example, in terms of agriculture, the exchangeable potassium content of about 170 mg/kg of soil is considered optimal while less or more than this amount may lead, respectively, to poor soil quality or environmental hazards (Karlen et al. 1994).

During last decades, several studies have shown that most soil properties including soil nutrients are continuous variables and have a tendency to change gradually (Tabor et al. 1985; Trangmar et al. 1985; Mulla 1991; Wollenhaupt et al. 1994; Goovaerts 1998; Western et al. 1998; Delbari et al. 2011; Vasu et al. 2017; Ma et al. 2017). Geostatistics provides a set of useful tools for quantitatively and qualitatively characterizing the spatial variability (via semivariogram) and estimation of soil attribute values at unsampled locations (using kriging). The geostatistical approaches are well known for their capability of modeling spatial variability of soil properties and their associated uncertainty which result in a reliable and comprehensive network of soil information for the sustainable management of agricultural lands on either a field or regional scale (Goovaerts 1999; Delbari et al. 2009; Delbari et al. 2010). This could finally result in higher quality and

quantity of agricultural productions and lower environmental hazards (Amini et al. 2005). A number of interpolation methods such as inverse distance weighing (IDW), ordinary kriging (OK), log kriging (LOK), and cokriging (COK) are used by several researchers to predict the spatial distribution of chemical, physical, and biological properties on the field and regional scales (Brouder et al. 2005; Kravchenko and Bullock 1999; Robinson and Metternicht 2006; Bogunovic et al. 2017; Delbari et al. 2011; Rosemary et al. 2017). Each of these methods can be more efficient in terms of soil characteristics, sample densities, number of samples, data distribution pattern, and natural conditions governing the study field (Brouder et al. 2005; Gotway et al. 1996; Laslett et al. 1987). IDW can be used to map the spatial distribution of any soil property measured for spatially distributed samples (Burgess and Webster 1980). A higher distance weighting power may result in a significant improvement of estimation accuracy (Kravchenko and Bullock 1999). Among kriging variants, OK provides the "best linear unbiased estimate" of a regionalized variable at unsampled locations, where "best" is defined in a least squares sense, as it aims to minimize the variance of estimation error (Goovaerts 1997). OK, however, may not provide the optimum result for a highly skewed data distribution. In such cases, an appropriate transformation function should be used beforehand. Moreover, if the property of interest is sparsely sampled or poorly correlated in space, its estimation could be improved by COK taking into account secondary variable(s) (Goovaerts 1998). Geypens et al. (1999) investigated the spatial variability of foil fertility parameters (i.e., P, K, Ca, Mg, and Na) in fields of different land use, in a Gleyic Podzol of Belgium. They found different ranges of spatial correlation for selected soil parameters indicating that a different sampling strategy should be adapted to the different soil parameters and the soil use. Cotway (1996) showed that for two elements of soil organic matter (OM) and nitrogen (N), IDW was better than the kriging method. Sun et al. (2003) evaluated the temporal and spatial variations of some soil quality properties and reported that soil properties exhibit a high amount of statistical variance. The highest and lowest amounts of the coefficient of variation were seen for phosphorus and pH, respectively. Statistical analysis showed that all soil properties (pH, OM, available phosphorus (AP), and available potassium (AK)) exhibit a degree of spatial correlation. The ratio of "nugget to sill" indicated a strong spatial correlation for pH and a moderate spatial correlation for other soil attributes. Robinson and Metternicht (2006) reported that OK and COK are appropriate methods for estimating soil electrical conductivity (EC) and organic matter while IDW is the best method for interpolating acidity (pH) in the southwest of Australia. Ayoubi et al. (2012) investigated the spatial variability of 14 soil physical and chemical properties in Sorkhonkhata region using geostatistical methods. Their results showed a moderate spatial correlation for many of

soil properties. Bogunovic et al. (2017) successfully characterized the spatial variability of soil pH, OM, AP, and AK at both local and regional scales.

Sistan Plain, located in the southeast of Iran, is characterized by a low precipitation and high evaporation rate. As it is typical for soils in arid and semi-arid regions including Iran, soils in Sistan Plain are affected by high amounts of salt and sodium contents, which may adversely influence soil aggregation and structure and intensify soil erosion. Sistan Plain is also confronted by soil degradation and desertification caused by extreme wind erosion due to prolonged drought and existence of high speed "120-day" wind. However, growing population and their need for food supply as well as dependence of Sistan economy on agriculture have imposed a lot of pressure on soil and water resources. Therefore, the knowledge of the spatial variation of soil quality properties is needed for better management of soil and water resources and ensuring sustainable agricultural production over the study area. The objectives of this research were (i) to explore the interrelationship between soil physical and chemical properties and their vertical variation in two successive layers of a salt-affected soil and (ii) to map the spatial distribution pattern of underlying soil attributes and nutrients by comparing OK, IDW, and COK in a saline-sodic soil in Sistan Plain, southeastern Iran.

Methodology

Study area

The study area (30° 55′N latitude and 61° 31′E longitude) is a part of Sistan Plain located in Sistan and Baluchestan Provinces, roughly 25 km south of Zabol and approximately 14 km from the Afghanistan borders. It covers an area of about 85 ha and includes a set of experimental plots that are monitored for irrigation and soil nutrient balance. Geologically, Sistan Plain is an alluvial plain and has very gentle slopes (0.025%) from the southeast toward the northwest. The study area is about 480 m above sea level. Sistan Plain has a hot and dry climate. The long-term average annual temperature at the site is 22 °C with minimum and maximum temperatures of − 10 °C and 51 °C, respectively. The long-term (40 years) average annual rainfall and evaporation are 60.8 and 4820.54 mm, respectively. Helmand River, originating from Afghanistan, is the main source of irrigation in the Zabol irrigation district. The 120-day wind of Sistan is the strongest wind in Iran with a speed of up to 120 km per hour, which blows almost from late May to late September (about 4 months). The wind originates from the central deserts in Iran and blows in a fairly constant direction (mainly from south to north) to Sistan and Baluchestan Provinces.

The soils of Sistan Plain have low pedogenic development and are mostly Aridosols and Entisols (Mirakzehi et al. 2018). Sistan Plain was used to have very fertile soils and various agricultural productions. However, for many years, it is confronted with severe salinization and soil degradation due to frequent droughts and wind erosion. The major crops are wheat, barley, and corn, which are cultivated under conventional agricultural tillage.

Soil sampling and measurements

The soil was sampled at 123 sites on a relatively regular grid of about 70-m interval (Fig. 1). Regular sampling is proved to be more accurate in predicting spatial distribution than random sampling (Hirzel and Guisan 2002). The locations of the samples were determined using a differential global positioning system (GPS) unit. Samples were collected at the end of November 2014 before planting. At each site, 1 kg soil samples were taken from two depths: 0–15 cm and 15–30 cm. The samples were transferred to the laboratory, air dried, and then crushed to pass through a 2-mm sieve. The samples were analyzed for the physical and chemical properties including percentages of sand, silt, and clay contents, denoted as Sand, Silt, and Clay, by the hydrometer method (Gee and Bauder 1986), volumetric soil water content (WC) using a portable time domain reflectometer (TDR), Na concentration by a flame photometer, Ca and Mg concentrations by EDTA titration, organic carbon (OC) by the modified Walkley Black method (USDA-NRCS 1996), EC with a EC meter (Rhoades 1996), and pH with a pH meter (Thomas 1996). Gypsum percentage was determined by precipitation with acetone (US Salinity Laboratory Staff 1954), soil available phosphorous (AP) was measured by Olsen et al. (1954), and available potassium (AK) was estimated by the method of Schollenberger and Simon (1945) using a flame photometer. Additionally, at each site, undisturbed soil samples were obtained from both depths using 100-cm³ steel cores to determine soil bulk density (BD; Blake and Hartge 1986).

Statistical analysis and data transformation

Descriptive statistics including mean, variance, standard deviation, minimum, maximum, skewness, and kurtosis values were calculated for each soil property. To determine the interrelation between soil properties and sampling depths, Pearson correlation coefficients were computed. In order to achieve a proper interpretation of geostatistical interpolation, data frequency distributional should follow a normal distribution (Clark 1979; Goovaerts et al. 2005; McGrath et al. 2004). On the other hand, the deviation from the normal distribution will affect the stability of the variance and hence semivariogram. Therefore, the normal distribution of raw data was investigated by Kolmogorov-Smirnov (K.S.) test. In
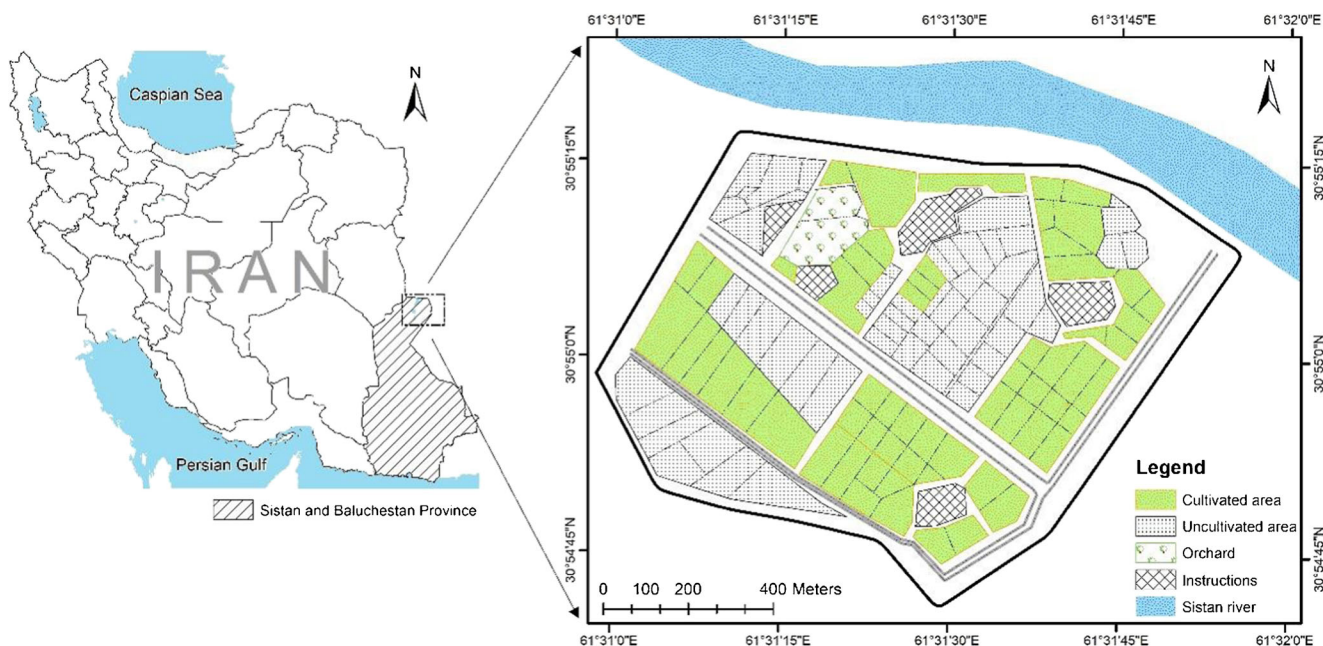
Fig. 1 Location of sampling points and land use map of study field

cases where the data were not normally distributed, two logarithmic and Box-Cox transformations were used to normalize the data (Fu et al. 2010; Thayer et al. 2003). Logarithm transform is used for the positively skewed distributions (McGrath et al. 2004). Box-Cox is a more powerful, widely used transformation when logarithm transform is not appropriate, e.g., for negatively skewed distributions (Box and Cox 1964; Gallardo and Paramá 2007). All the statistical tests were performed using the SPSS statistical software, version 11.0 (Norušis 2002).

Geostatistical analysis

The first step of a geostatistical analysis is to investigate the spatial continuity of underlying soil property. The (cross) semivariograms functions describe the spatial (cross) correlation between data values (Isaaks and Srivastava 1989). Suppose $z(u_i)$, $i = 1,…, n$ represents the values of a soil attribute at n sampling locations. The experimental (cross) semivariograms are calculated using the following equation:

$$\gamma_{vw}^{*}(h) = \frac{1}{2N(h)}$$
$$\times \sum_{i=1}^{N(h)} \left\{ [z_v(u_i + h) - z_v(u_i)][z_w(u_i + h) - z_w(u_i)] \right\}$$

(1)

where γ_{vw}^{*} is the experimental semivariogram when $v = w$ and cross-semivariogram when $v \neq w$ and $N(h)$ is the number of pairs of regionalized variables $z_v(u_i)$ and $z_w(u_i)$ at a given separation distance h. To obtain (cross) semivariogram value for any given h, a theoretical model should be fitted to the experimental values. The theoretical semivariogram models applied in this study were often either a spherical (Eq. 2) or an exponential (Eq. 3) model (Isaaks and Srivastava 1989; Goovaerts 1997):

$$\gamma(h) = \begin{cases} C_0 + C\left[\frac{3}{2}\frac{h}{a} - \frac{1}{2}\left(\frac{h}{a}\right)^3 \right] & for\ h \leq a \\ C_0 + C & otherwise \end{cases}$$

(2)

$$\gamma(h) = C_0 + C\left(1 - \exp\left(-\frac{3h}{a}\right)\right)$$

(3)

where C_0 is the nugget effect, C is the partial sill, and a is the practical range (for exponential model practical range is the value of h when h reaches 95% of the sill value). The nugget effect often arises from a combination of measurement errors and small-scale spatial variation (Journel and Huijbregts 1978). The semivariogram model and its parameters are then used to estimate the soil properties at unobserved locations through ordinary (log) kriging and cokriging.

Ordinary kriging (OK) predicts the value of a soil property at an unsampled location, $\hat{z}(u_0)$, as a linear weighted average of $n(u_0)$ neighboring observations (Goovaerts 1997):

$$\hat{z}(u_0) = \sum_{i=1}^{n(u_0)} \lambda_i z(u_i) \quad with \quad \sum_{i=1}^{n(u_0)} \lambda_i = 1$$

(4)

where λ_i are the ordinary kriging weights that minimize the estimation variance and provide an unbiased estimator, i.e., $E\{\hat{z}(u_0) - z(u_0)\} = 0$. The weights λ_i are determined through the following OK system:

$$\begin{cases} \sum_{j=1}^{n(u_0)} \lambda_j \gamma(u_i, u_j) + \mu = \gamma(u_i, u_0) & i = 1, ..., n(u_0) \\ \sum_{j=1}^{n(u_0)} \lambda_j = 1 \end{cases} \quad (5)$$

where μ is the Lagrange multiplier.

The OK estimation variance is computed as follows:

$$\sigma^2 = \sum_{i=1}^{n} \lambda_i \gamma(u_i, u_0) + \mu \quad (6)$$

If a normal distribution of errors is assumed, OK variance corresponding to each estimate can be used to generate a confidence interval for that estimate (Goovaerts 1997).

OK does not require the data to have a normal distribution; however, OK predictor performs better if data histogram is not highly skewed. Normalizing the data distribution suppresses outliers and improves data stationarity. Log-normal transform is commonly used to symmetrize the distribution, and OK is then performed on log-normal transforms of the observed values.

The cokriging (COK) estimator $\hat{z}_v(u_0)$ at unsampled location u_0, assuming that there is one auxiliary variable z_w cross-correlated with the main variable z_v, is given as (Isaaks and Srivastava 1989)

$$\hat{z}_v(u_0) = \sum_{i=1}^{n(u_0)} \alpha_i \cdot z_v(u_i) + \sum_{j=1}^{m(u_0)} \beta_j \cdot z_w(u_j) \quad (7)$$

where α_i and β_j are the weights assigned to the known values of the primary and secondary variables z_v and z_w, respectively, and $n(u_0)$ and $m(u_0)$ are the number of primary and secondary observations. Like for OK, the COK estimator is required to be unbiased and have a minimum variance of errors. To obtain an unbiased estimator, the sum of weights α_i should be unity while the sum of weights β_j should be zero (Goovaerts 1997).

For COK, a linear model of co-regionalization with an isotropic spherical model is used to describe the spatial variability. In cases where both exponential and spherical models may be successfully fitted to the experimental semivariograms, the spherical model is considered to be more effective ensuring semi-positive definiteness (Goulard and Voltz 1992).

In this study GS+ software (Robertson 2008) was used to compute experimental semivariograms and to find the best fitted theoretical model to the experimental points considering the highest regression coefficient (r^2) and the least residual sum of squares (RSS) values. The spatial interpolation of soil properties and mapping were performed within the spatial analyst extension module in ArcGis 10.2.

Evaluation of estimation methods

A cross-validation technique (Isaaks and Srivastava 1989) was applied to evaluate the performance of the estimation approaches used. The cross-validation test includes removing one observed value from the dataset and then estimating the value at that location using the remaining data through each interpolator. The validation criteria used are given as follows:

$$MBE = \frac{1}{n} \sum_{i=1}^{n} (z(u_i) - \hat{z}(u_i)) \quad (8)$$

$$MAE = \frac{1}{n} \sum_{i=1}^{n} |(z(u_i) - \hat{z}(u_i))| \quad (9)$$

$$RMSE = \frac{1}{n} \sum_{i=1}^{n} (z(u_i) - \hat{z}(u_i))^2 \quad (10)$$

where $z(u_i)$ and $\hat{z}(u_i)$ are the observed and estimated soil properties, respectively, at any location i. These statistics determine the closeness of the estimated values to observed values. An appropriate interpolation method should have an MBE close to zero, less amount of MAE and RMSE, and a correlation coefficient (R) close to 1.

Results and discussion

Statistical analysis

A summary statistics of soil properties is given in Table 1. The mean values for Na, Mg, and Ca as well as EC in 0–15 cm are more than those in 15–30 cm, which means that salts are accumulated in surface layer mainly due to the high amount of evaporation from the soil surface and low precipitation. Soil texture fractions are almost the same in terms of their mean values. The soil texture contains approximately 50% Sand, 30% Silt, and 20% Clay, and the dominant soil texture classes are sandy loam and loam according to the soil texture triangle defined by USDA (Soil Science Division Staff 2017). As seen in Table 1, the whole field is low to medium in organic carbon; OC ranges from 0.37 to 3.31(%) with a mean value of about 2%. The low concentration of OC in topsoil (0–30 cm) is expected in hot and arid regions due to high evaporation and wind erosion (Salem 1989), and low primary production (Ontl and Schulte 2012).

As shown in Table 1, all the samples are alkaline in reaction, and strongly calcareous in nature. For several samples selected randomly within the study area, the percent of Lime was also measured. The results (not shown) indicated that all samples have a high amount of Lime (about 39% on average) for both depths. The high level of Lime in Aridisols and Entisols orders is common. Lime increases the biological activity of the soil; however, it may cause carbonation or environmental impact (Jawad et al. 2014). Excessive lime creates a hard layer in the soil and, as a result, provides unfavorable

Table 1 Descriptive statistics of soil properties in depths of 0–15 cm and 15–30 cm

Variable	Depth (cm)	Maximum	Mean	Minimum	Standard deviation	Coefficient of variation (%)
Sand (%)	0–15	71.88	48.58	20	12.13	24.95
	15–30	83.76	49.54	19.2	13.38	27
Clay (%)	0–15	37.2	20.53	10.4	5.54	26.98
	15–30	65.8	20.13	8	7.41	36.81
Silt (%)	0–15	50.2	30.88	5.6	9.33	30.21
	15–30	57.2	30.52	9.6	10.71	35
BD (gr/cm^3)	0–15	1.72	1.42	1.14	0.10	6.98
	15–30	1.71	1.53	1.18	0.09	6.13
WC (%)	0–15	39	13.52	2.1	7.47	55.25
	15–30	35.1	16.06	2.3	7.86	48.94
EC (dS/m)	0–15	34	3.66	0.72	5.54	151.36
	15–30	17.19	2.18	0.49	2.71	124.31
ESP (%)	0–15	22.14	3.46	0.38	3.54	102.31
	15–30	20.96	3.08	0.082	2.99	97.07
SAR	0–15	20.14	3.14	0.85	2.57	81.84
	15–30	18.84	3.00	0.47	2.33	77.67
pH	0–15	8.95	8.5	7.96	0.21	2.47
	15–30	8.86	8.48	7.8	0.20	2.35
Na (mg/kg)	0–15	92.06	10.94	1.25	17.33	158.4
	15–30	61.39	7.19	1.40	8.90	123.75
Ca (mg/kg)	0–15	26	5.68	1.4	4.44	78.16
	15–30	13.4	3.45	0.8	2.16	62.59
Mg (mg/kg)	0–15	41.6	7.74	0.8	7.53	97.28
	15–30	31.2	5.09	0.4	5.30	104.11
OC (%)	0–15	3.31	2.08	0.37	0.63	30.28
	15–30	3.29	1.84	0.29	0.60	32.4
Gypsum (%)	0–15	38.99	16.81	8.50	4.95	29.44
	15–30	58.43	32.01	17.12	7.26	22.68
AP[a] (ppm)	0–15	148.67	45.02	3.71	52.71	117
AK[a] (ppm)	0–15	448.00	163.76	80.00	60.29	36.82

[a] AP and AK were only measured in the topsoil

conditions for the absorption of some nutrients by the plant. The use of sulfuric acid and other acidifying substances in calcareous soils can increase the solubility of the micronutrients, such as P, Fe, Mn, Zn, and Cu, since it removes soil bicarbonate from the soil and lower soil pH. Table 1 also shows that both layers contain high amount of gypsum, which is a common component in arid and semi-arid areas. However, the mean value of gypsum for subsoil (32.01%) is roughly two times greater than that for topsoil (16%). That means gypsum is moved downward by irrigation water and deposited in deeper layers. Gypsum in small percentage is useful for plant growth as it tends to prevent the formation of an alkali soil. However, a high quantity of gypsum causes low crop yield due to unbalanced uptake of nutrients by the plant roots (Van Alphen and de los Ríos Romero 1971). According to a classification proposed by Warrick

(1998), Na, Mg, Ca, WC, EC, ESP, SAR, and AP have a large coefficient of variation (CV) (more than 50%) for both depths and Sand, Silt, Clay, OC, AK, and gypsum have a moderate CV (between 25 and 50%). Low CV (less than 15%) was seen for BD and pH. Low CV for pH in agricultural soil is reported by many researchers (McBratney and Webster 1983; Boekhold and Van der Zee 1992; Chung et al. 1995; Bhatti et al. 1999; Bogunovic et al. 2017; Vasu et al. 2017; Rosemary et al. 2017). Vasu et al. (2017) and Rosemary et al. (2017) also reported a moderate CV for OC. Rosemary et al. (2017) reported a high CV for EC and a moderate CV for Silt and Clay. Na and EC similarly have the highest CV values (> 150%) for both depths, meaning a large variability of these properties across the study area. The high variation of salinity could be due to anthropogenic factors such as land use and irrigation (Zhang et al. 2014).

It is natural not to follow a normal distribution for some soil data, as mentioned by McGrath and Zhang (2003). However, to achieve a better interpretation of geostatistical analyses, data distribution should at least follow a distribution near-normal distribution (Zhang 2006). As seen in Table 1, the values of skewness are very small for BD and soil texture fractions except for clay content in the deeper layer. WC and OC in topsoil, Ca in the subsoil, and Na, Mg, EC, ESP, and gypsum in both topsoil and subsoil are strongly positively skewed while pH is negatively skewed. The natural logarithm is used to transform the frequency distribution of positively skewed variables (except for EC and Na) to a nearly normal distribution before using geostatistical analysis (Table 2). A weighted technique, which can approximate true population statistics more closely (Haan 2002), is used to back transform the data, afterward. For EC and Na, Box-Cox transform is used to normalize the data distribution (Table 2).

The Pearson correlation coefficients between the pairs of soil properties are calculated and presented in Table 3. As seen, there are statistically ($p < 0.01$ and $p < 0.05$) significant correlations between some soil physical and chemical properties at topsoil and subsoil. The existence of such a positive and negative correlation between soil physical and chemical characteristics allows us to take advantage of multivariate interpolation methods such as COK. Soil texture fractions and especially Sand and Silt have a statistically significant ($p < 0.01$) positive or negative correlation with many of soil properties such as WC, EC, ESP, Na, OC, and AK for 0–15-cm depth. These relations decreased for the subsoil. There is a high statistically

significant ($p < 0.01$) correlation between EC and ESP, SAR, pH, Na, Ca, Mg, gypsum, and AK for topsoil. EC is also correlated ($p < 0.01$) to ESP, SAR, pH, Na, Ca, and Mg at subsoil. Topsoil pH has a significant ($p < 0.01$) negative relation with SAR, ESP, EC, Na, Ca, Mg, and gypsum. However, pH was only significantly ($p < 0.01$) negatively related to EC, Na, Ca, and Mg at subsoil. The results also showed a significant negative correlation between OC and Sand ($r = -0.363$, $p < 0.01$) and positive correlation between OC and Silt ($r = 0.362$, $p < 0.01$), and Clay (0.174, $p < 0.05$) for topsoil. Similarly, OC is correlated negatively with Sand ($r = -0.435$, $p < 0.01$), and positively with Clay ($r = 0.456$, $p < 0.01$), Silt ($r = 0.22$, $p < 0.01$), and WC ($r = 0.283$, $p < 0.01$) for subsoil. The fact that OC is positively correlated with percent Clay is also reported by Adhikari and Bhattacharyya (2015), Nichols (1984), Safadoust et al. (2016a), and Sakin (2012a). Our finding confirms that of Adhikari and Bhattacharyya (2015) and MacCarthy et al. (2013), who found a negative correlation between Sand and OC. However, Sakin (2012b) stated that Sand is positively correlated with OC. MacCarthy et al. (2013) reported a negative correlation between OC and BD. Evrendilek et al. (2004) reported a positive correlation between OC and the amount of moisture available to the soil and a negative correlation between OC and BD as well as soil pH. As seen in Table 3, except for OC, the correlation between soil properties decreased with depth. The higher amount of statistically ($p < 0.01$ and $p < 0.05$) significant correlation with other properties belong to Silt, WC, EC, ESP, Na, and gypsum in topsoil and Sand, EC, and OC in subsoil.

Table 2 Kolmogorov-Smirnov statistics for soil properties before and after transformation

	Topsoil (0–15 cm)				Subsoil (15–30 cm)			
	Transform	Skewness	Kurtosis	P (K-S)	Transform	Skewness	Kurtosis	P (K-S)
Sand (%)	–	− 0.072	− 0.76	0.735	–	− 0.106	− 0.431	0.822
Clay (%)	–	0.524	0.076	0.174	log	0.106	1.045	0.442
Silt (%)	–	− 0.004	− 0.572	0.725	–	0.316	− 0.359	0.429
BD (gr/cm^3)	–	0.041	0.693	0.90	–	− 0.578	0.958	0.697
WC (%)	log	− 0.215	− 0.27	0.737	–	0.387	− 0.783	0.385
EC (dS/m)	Box-Cox	0.044	− 0.591	0.44	Box-Cox	0.109	0.336	0.741
ESP (%)	log	0.821	1.68	0.326	log	− 0.351	3.24	0.376
SAR	log	0.94	3.510		log	0.81	2.92	
pH	–	− 0.844	− 0.064	0.113	–	− 0.898	1.081	0.428
Na (mg/kg)	Box-Cox	− 0.164	0.993	0.115	Box-Cox	0.002	0.931	0.535
Ca (mg/kg)	–	0.663	− 0.045	0.06	log	0.562	0.893	0.09
Mg (mg/kg)	log	0.494	0.245	0.211	log	0.487	1.711	0.132
OC (%)	log	− 0.56	− 0.049	0.852	–	0.22	− 0.306	0.847
Gypsum (%)	log	0.48	0.31	0.109	log	0.15	0.55	0.06
AP (ppm)	log	0.54	− 0.93		–	–	–	–
AK (ppm)	log	0.54	0.48		–	–	–	–

Table 3 Linear correlation coefficients between soil physical and chemical properties

0–15 (cm)	Sand (%)	Clay (%)	Silt (%)	BD (gr/cm³)	WC (%)	EC (dS/m)	ESP (%)	SAR	pH	Na (mg/kg)	Ca (mg/kg)	Mg (mg/kg)	OC	Gypsum (%)	AP
Sand (%)	1														
Clay (%)	−0.674**	1													
Silt (%)	−0.899**	0.282**	1												
BD (gr/cm³)	−0.088	0.134	0.035	1											
WC (%)	−0.448**	0.356**	0.366**	0.200**	1										
EC (dS/m)	−0.263**	0.050	0.313**	0.067	0.242*	1									
ESP (%)	−0.305**	0.107	0.359**	0.0493	0.394**	0.831**	1								
SAR	−0.305**	0.011	0.331**	0.071	0.387**	0.833**	0.998**	1							
pH	0.086	0.098	−0.170*	0.060	−0.117	−0.520**	−0.471**	−0.468**	1						
Na (mg/kg)	−0.311**	0.092	0.350**	0.077	0.390**	0.908**	0.944**	0.945**	−0.560**	1					
Ca (mg/kg)	−0.125	−0.063	0.259**	0.034	−0.020	0.647**	0.572**	0.576**	−0.420**	0.740**	1				
Mg (mg/kg)	−0.113	−0.014	0.11	0.081	0.005	0.637**	0.523**	0.513**	−0.510**	0.670**	0.904**	1			
OC (%)	−0.363**	0.174*	0.362**	0.031	0.206*	0.096	0.080	0.065	−0.029	0.083	0.196*	0.141	1		
Gypsum (%)	−0.162	−0.027	0.225*	0.125	0.234*	0.521**	0.516**	0.500**	−0.366**	0.504**	0.429**	0.470**	0.162*	1	
AP (ppm)	−0.098	−0.021	0.140	0.134	0.098	−0.118	−0.022	−0.018	0.121	−0.022	−0.009	−0.116	0.038	0.096	1
AK (ppm)	0.364**	0.348**	0.267**	0.058	0.340**	0.259**	0.265**	0.254*	−0.180*	0.333**	0.406**	0.402**	0.177*	0.186*	0.021
15–30 (cm)															
Sand (%)	1														
Clay (%)	−0.640**	1													
Silt (%)	−0.827**	0.084	1												
BD (gr/cm³)	0.056	0.095	−0.149	1											
WC (%)	−0.448**	0.307**	0.345**	0.190*	1										
EC (dS/m)	−0.184*	0.121	0.155	−0.022	0.235*	1									
ESP (%)	−0.159*	0.194*	0.052	0.006	0.107	0.610**	1								
SAR	−0.169*	0.197*	0.065	0.009	0.111	0.613**	0.997**	1							
pH	0.072	−0.057	−0.064	0.120	−0.091	−0.411**	−0.089	−0.071	1						
Na (mg/kg)	−0.237*	−0.301*	−0.080	−0.022	−0.181	0.856**	0.750**	0.734**	−0.337**	1					
Ca (mg/kg)	−0.214*	0.044	0.232*	−0.128	0.035	0.504**	0.153	0.148	−0.366**	0.478**	1				
Mg (mg/kg)	−0.113	−0.043	0.154	−0.073	0.096	0.637**	0.102	0.095	−0.506**	0.530**	0.550**	1			
OC (%)	−0.435**	0.456**	0.220**	0.014	0.283**	0.131	0.214*	0.231*	0.062	0.192*	0.068	0.011	1		
Gypsum (%)	−0.116	0.124	0.040	−0.023	−0.045	0.182*	0.142	0.140	−0.212*	0.285*	0.143	0.215*	−0.041	1	

**Correlation is significant at the 0.01 level (two-tailed). *Correlation is significant at the 0.05 level (two-tailed)

Geostatistical analysis

Autocorrelation analysis

Experimental semivariograms are first calculated for each soil property for both depths 0–15 cm and 15–30 cm. Then the best theoretical model is fitted to the experimental values considering the goodness of fit in terms of the regression coefficient (r^2) and the RSS through a trial-and-error procedure. In general, for both depth intervals, the studied soil properties showed a moderate (M) to strong (S) spatial auto-correlation with either a spherical or an exponential semivariogram model. However, the radius of spatial continuity was quiet small for some soil properties such as AP; it was almost equal to sampling distance (70 m). This dictates a low spatial continuity of AP, which is mainly due to the intrinsic variability of soil (Cambardella et al. 1994). One of the most important issues that matter in soil heterogeneity is the role of natural (internal) and external factors on spatial auto-correlation of soil properties in different depths. For example, spatial variability of soil physical properties such as soil structure and BD in topsoil is highly controlled by soil management practices, e.g., soil tillage and plowing (Gomez et al. 2005). However, soil operations, such as agriculture and other management activities in the surface soil, have little impact on physical properties of subsurface soil.

To investigate the anisotropy of the studied properties, their experimental semivariograms were calculated for four directions 0, 45, 90, and 135° with an angle tolerance of 22.5°. No significant anisotropy was observed within the spatial correlation radius. This means that the spatial correlation of soil properties is mainly a function of the distance between pairs of samples; so omni-directional semivariogram was used for further analyses. According to Table 4, soil texture fractions (Sand, Clay, and Silt) exhibited a moderate to strong continuity in space with a spherical model of spatial structure. The greatest spatial correlation distance was seen for soil texture (up to 800 m). However, Sand and Clay showed higher spatial autocorrelation than Silt in terms of effective range and the C_0/Sill ratio (Table 4). Delbari et al. (2011) reported a high spatial correlation for Sand and Silt and a moderate spatial correlation for Clay with a spherical structure for all fractions in an agriculture field in Lower Austria. Stronger spatial dependencies are controlled by the intrinsic variability of soil (Cambardella et al. 1994). Rosemary et al. (2017) reported a moderate and strong spatial correlation for Clay and Sand, respectively. They reported a spherical spatial structure with spatial correlation distances of 200 m and 290 m for Clay and Sand, respectively. Iqbal et al. (2005) found a moderate spatial correlation of Sand and Clay with an exponential structure in an alluvial floodplain soil. The BD experimental semivariogram showed a moderate spatial correlation and a spherical structure. Iqbal et al. (2005) also reported a moderate

spatial correlation of BD. However, the spatial structure of BD followed an exponential model with a smaller radius of influence in different soil horizons.

As seen in Table 4, EC showed a moderate spatial correlation with a spherical model of the spatial structure for both depths. The effective range for EC was 190 m and 175 m for 0–15 and 15–30 cm, respectively. Rosemary et al. (2017) reported a spherical structure with a range of influence 830 m for EC in depth 0–30 cm. However, Walter et al. (2001) used an exponential model to describe the spatial structure of surface soil salinity. In this study, a strong and moderate spatial continuity was found for topsoil and subsoil pH, respectively. The range of influence was nearly 150 m for both depth intervals. Cemek et al. (2007) reported an exponential model of the spatial structure with an effective range of 1340 m for pH and a spherical spatial structure with an effective range of 3420 and 3700 m for EC and ESP, respectively. In a study by Huang et al. (2001), pH experimental semivariogram followed a spherical model with a range of about 260 m for both 0–5-cm and 5–10-cm soil depths. Shukla et al. (2004) reported a moderate spatial correlation for Silt, Clay, BD, and EC and a weak spatial continuity for pH at topsoil (0–15 cm). Rosemary et al. (2017) used a spherical model with a range of influence 590 m for describing the spatial structure of pH in 0–30-cm depth.

The range of influence for most soil properties was greater than sampling distance (often more than two times), indicating that the sampling interval used in this study is sufficient. Kerry and Oliver (2004) pointed out that the sampling distance for future researches should be less than half the effective range. However, AP and subsoil ESP showed a small range of influence (about 70 m). The strong spatial dependence of soil properties may be controlled by soil intrinsic variability while the weak spatial correlation could be attributed to the external factors (Cambardella et al. 1994; Geypens et al. 1999). The difference in spatial variability of soil properties could be related to the forming processes of soil as well as land and water management practices (Abegaz and Adugna 2015).

For the application of the COK method for those variables with a weaker spatial continuity, the experimental semivariogram of the auxiliary variables and cross-semivariogram between the main and auxiliary variable were calculated and modeled. The main characteristics of the fitted models are given in Table 4. As shown, either a spherical or an exponential model found to have the best fit to the experimental cross-semivariograms.

Spatial interpolation and mapping of soil properties

The cross-validation results of estimating soil properties using (log) OK, IDW, and COK are presented in Table 5. In terms of MAE, RMSE, and R, IDW often resulted in a slightly smaller estimation error for estimating Sand, Silt, Clay, Mg, and AP.

Table 4 Characteristics of the best model fitted to experimental (cross) semivariogram for soil properties in depths 0–15 cm and 15–3 cm

Variable	Soil depth (cm)	Semivariogram model	Nugget effect	Sill	Effective range (m)	$C_0/(C_0 + C)$ [class]	r^2	RSS
Sand (%)	15–0	Spherical	55.1	150.2	650	0.37 [M]	0.962	563
	30–15	Spherical	59.5	193.5	760	0.31 [M]	0.943	713
Clay (%)	15–0	Spherical	9.96	35.51	760	0.28 [M]	0.929	34.7
	30–15	Spherical	0.05	0.125	835	0.40 [M]	0.929	0.0002
Silt (%)	15–0	Spherical	37.1	93.0	620	0.40 [M]	0.952	147
	30–15	Spherical	48.3	107	620	0.45 [M]	0.860	443
BD (gr/cm^3)	15–0	Spherical	0.0068	0.01	540	0.68 [M]	0.749	0.0001
	30–15	Spherical	0.0043	0.008	610	0.54 [M]	0.840	0.0001
WC (%)	15–0	Exponential	0.024	0.316	300	0.08 [S]	0.958	0.001
	30–15	Exponential	6.3	61.66	230	0.10 [S]	0.835	142
EC (dS/m)	15–0	Spherical	0.35	0.77	190	0.45 [M]	0.896	0.007
	30–15	Spherical	0.25	0.50	175	0.50 [M]	0.831	0.003
ESP (%)	15–0	Exponential	0.22	0.44	250	0.49 [M]	0.87	0.002
	30–15	Exponential	0.3	0.565	72	0.53 [M]	0.616	0.032
SAR	15–0	Exponential	0.002	0.274	180	0.01 [S]	0.872	0.002
	30–15	Exponential	0.012	0.280	120	0.04 [S]	0.577	0.003
pH	15–0	Spherical	0.009	0.054	150	0.16 [S]	0.713	0.001
	30–15	Spherical	0.019	0.044	152	0.43 [M]	0.501	0.0002
Na (mg/kg)	15–0	Spherical	0.307	0.693	182	0.44 [M]	0.934	0.002
	30–15	Spherical	0.25	0.485	130	0.29 [M]	0.460	0.007
Ca (mg/kg)	15–0	Spherical	0.208	0.416	235	0.5 [M]	0.655	0.008
	30–15	Spherical	0.116	0.248	160	0.47 [M]	0.350	0.0004
Mg (mg/kg)	15–0	Spherical	0.266	0.650	165	0.41 [M]	0.825	0.009
	30–15	Spherical	0.244	0.491	150	0.49 [M]	0.586	0.004
OC (%)	15–0	Spherical	0.25	0.42	400	0.60 [M]	0.590	0.010
	30–15	Spherical	0.26	0.37	400	0.70 [M]	0.680	0.004
Gypsum (%)	15–0	Exponential	0.027	0.074	185	0.36 [M]	0.843	0.0002
	30–15	Spherical	0.022	0.05	140	0.44 [M]	0.617	0.0001
AP (ppm)	0–15	Spherical	0.027	1.226	70	0.02 [S]	0.045	0.019
AK (ppm)	0–15	Spherical	0.065	0.122	700	0.53 [M]	0.928	0.0002
WC-Sand	15–0	Spherical	− 0.013	− 0.068	650	0.19 [S]	0.902	0.0004
WC-Clay	30–15	Gaussian	3.05	21.12	690	0.14 [S]	0.740	160
EC-Na	15–0	Exponential	0.001	0.584	204	0.00 [S]	0.858	0.014
ESP-Na	15–0	Exponential	0.001	0.485	204	0.00 [S]	0.889	0.007
ESP-Na	30–15	Exponential	0.1	0.42	135	0.00 [S]	0.375	0.0001
pH-Na	15–0	Exponential	− 0.07	− 0.12	180	0.58 [M]	0.280	0.0025
OC-Sand	0–15	Spherical	− 0.30	− 3.10	600	0.10 [S]	0.852	1.40
OC-Clay	30–15	Spherical	0.03	0.115	700	0.26 [M]	0.610	0.002
Gypsum-Na	0–15	Spherical	0.04	0.089	280	0.45 [M]	0.679	0.0004
Gypsum-Na	15–30	Spherical	0.02	0.043	130	0.47 [M]	0.579	0.003
AK-Sand	15–0	Spherical	0.4	− 1.70	650	0.24 [S]	0.816	1.26

However, the bias (MBE) was smaller for OK. Also, for BD and pH for two layers, subsoil EC and OC as well as topsoil AK, both OK and IDW performed very similar. For estimating topsoil WC, IDW (RMSE = 6.40%, MBE = 0.131%) was the best interpolator; however, there was not a significant difference between selected interpolators for estimating subsoil WC (Table 5). The results indicated that OK performed slightly better for estimating ESP, SAR, Na, Ca, and topsoil EC. COK with the auxiliary variable Clay slightly improved the accuracy of estimating topsoil OC. However, COK was

Table 5　Cross-validation results of estimating soil properties by OK, IDW, and COK

Variable	Depth (cm)	(Log) OK				IDW				COK			
		R	MBE	MAE	RMSE	R	MBE	MAE	RMSE	R	MBE	MAE	RMSE
Sand (%)	15–0	0.64	− 0.085	7.268	9.278	0.64	− 0.26	7.133	9.239				
	30–15	0.64	− 0.144	7.833	10.30	0.66	− 0.53	7.668	10.06				
Clay (%)	15–0	0.61	0.042	3.345	4.368	0.63	0.09	3.314	4.304				
	30–15	0.50	0.177	4.18	6.45	0.48	0.268	4.3	6.48				
Silt (%)	15–0	0.57	0.09	5.94	7.611	0.58	0.262	5.827	7.565				
	30–15	0.59	0.261	6.3	8.457	0.59	0.434	6.258	8.396				
BD (gr/cm^3)	15–0	0.36	0.0	0.076	0.092	0.38	0.0	0.077	0.091				
	30–15	0.50	0.0	0.06	0.081	0.51	0.0	0.061	0.081				
WC (%)	15–0	0.51	0.208	4.815	6.41	0.52	0.131	4.709	6.40	0.492	0.527	4.918	6.505
	30–15	0.50	0.189	5.586	6.80	0.47	0.199	5.595	6.90	0.472	0.033	5.538	6.87
EC (dS/m)	15–0	0.240	− 0.25	2.26	5.42	0.203	− 1.34	2.47	5.63	0.220	0.61	3.62	6.32
	30–15	0.103	− 0.11	1.48	2.71	0.102	− 0.58	1.35	2.76				
ESP (%)	15–0	0.29	− 0.08	1.330	3.374	0.22	0.07	1.941	3.473	0.26	0.05	1.908	3.485
	30–15	0.22	0.253	2.028	3.23	0.17	0.012	1.898	3.247	0.16	0.377	2.054	3.252
pH	15–0	0.29	− 0.00	0.172	0.217	0.264	− 0.00	0.173	0.219	0.31	− 0.00	0.171	0.216
	30–15	0.348	0.003	0.143	0.193	0.324	0.006	0.143	0.192				
SAR	15–0	0.384	0.02	0.83	1.57	0.326	− 0.19	0.82	1.62				
	30–15	0.068	0.02	0.91	1.50	0.02	− 0.2	0.89	1.50				
Na (mg/kg)	15–0	0.350	− 0.89	7.81	16.24	0.277	0.357	9.07	16.70				
	30–15	0.44	− 0.36	4.17	8.06	0.286	− 1.77	3.92	8.74				
Ca (mg/kg)	15–0	0.312	0.146	2.719	4.182	0.311	0.058	2.726	4.193				
	30–15	0.310	0.15	1.31	2.06	0.329	− 0.32	1.18	2.05				
Mg (mg/kg)	15–0	0.281	0.058	4.807	7.229	0.334	0.069	4.768	7.159				
	30–15	0.223	0.066	2.99	5.15	0.226	− 1.64	2.57	5.25				
OC (%)	15–0	0.45	0.008	0.454	0.562	0.44	− 0.01	0.45	0.564	0.54	0.004	0.39	0.485
	30–15	0.411	0.012	0.435	0.545	0.414	0.022	0.427	0.546	0.40	− 0.001	0.438	0.564
Gypsum (%)	15–0	0.36	0.53	3.59	4.64	0.36	− 0.46	3.37	4.62	0.363	0.92	3.75	4.61
	30–15	0.12	0.675	5.825	7.19	0.12	− 0.506	5.978	7.215	0.15	0.78	5.834	7.21
AP (ppm)	0–15	0.041	4.59	41.52	57.84	0.04	− 19	39.91	57.80				
AK (ppm)	0–15	0.42	2.02	37.80	56.95	0.43	− 1.94	36.87	56.84	0.35	− 0.03	41.96	62

not able to improve the estimation accuracy for WC, ESP, gypsum, topsoil EC, pH, and AK as well as subsoil OC. This could be due to low sampling density and low spatial continuity of co-variables, and lack of strong cross-relation between the primary and secondary variables. However, data transformation of skewed distributions slightly improved the spatial dependence and accuracy of interpolation.

Figure 2 shows the spatial distribution map of soil properties generated using the best interpolation method. The map of difference between two layers in terms of each attribute (subsoil minus topsoil) is also shown. According to the map of soil texture fractions, the spatial distribution patterns of Sand, Silt, and Clay are almost the same at both depths. The lowest amount of Sand is located on the southwest of the study field, and coarser soil texture is seen near the riverbank in north and northeastern areas. The least clay content is seen in the

northern part of the field and the least amount of silt is in the eastern part of field. As seen in Fig. 2, the percentage of soil fractions is changing slightly from topsoil to subsoil. For example, Sand content is decreasing (up to 26%) in, e.g., north and northeast of the study area, while it is increasing (up to 37%) in, e.g., southeast of the study field. In terms of BD, most of the field area contain a bulk density of less than 1.44 g/cm^3 at topsoil and greater than 1.44 g/cm^3 at subsoil, resulting in an increase of up to 0.2 g/cm^3 BD in subsoil, e.g., along the northeast to southeast of the study field. The increase of BD with soil depth is related to the less pore spaces in subsoil mostly due to more compaction, less organic matter, less aggregation, and less root penetration of subsurface compared to surface layers (Sakin 2012a, 2012b). Based on the maps of WC, the amount of topsoil water content is lower than subsoil water content. However, the spatial distributions of

WC in both depths are similar; the amount of WC is higher in cultivated areas where surface irrigation was applied (few weeks ahead of sampling), and less in drip irrigated orchards and non-irrigated areas (see Fig. 1). EC decreased from the surface layer to the subsurface layer which could be due to extreme evaporation rate, no precipitation, and poor surface drainage. The lowest amount of topsoil EC is seen in north, northeast, and southeast of study field with coarser soil
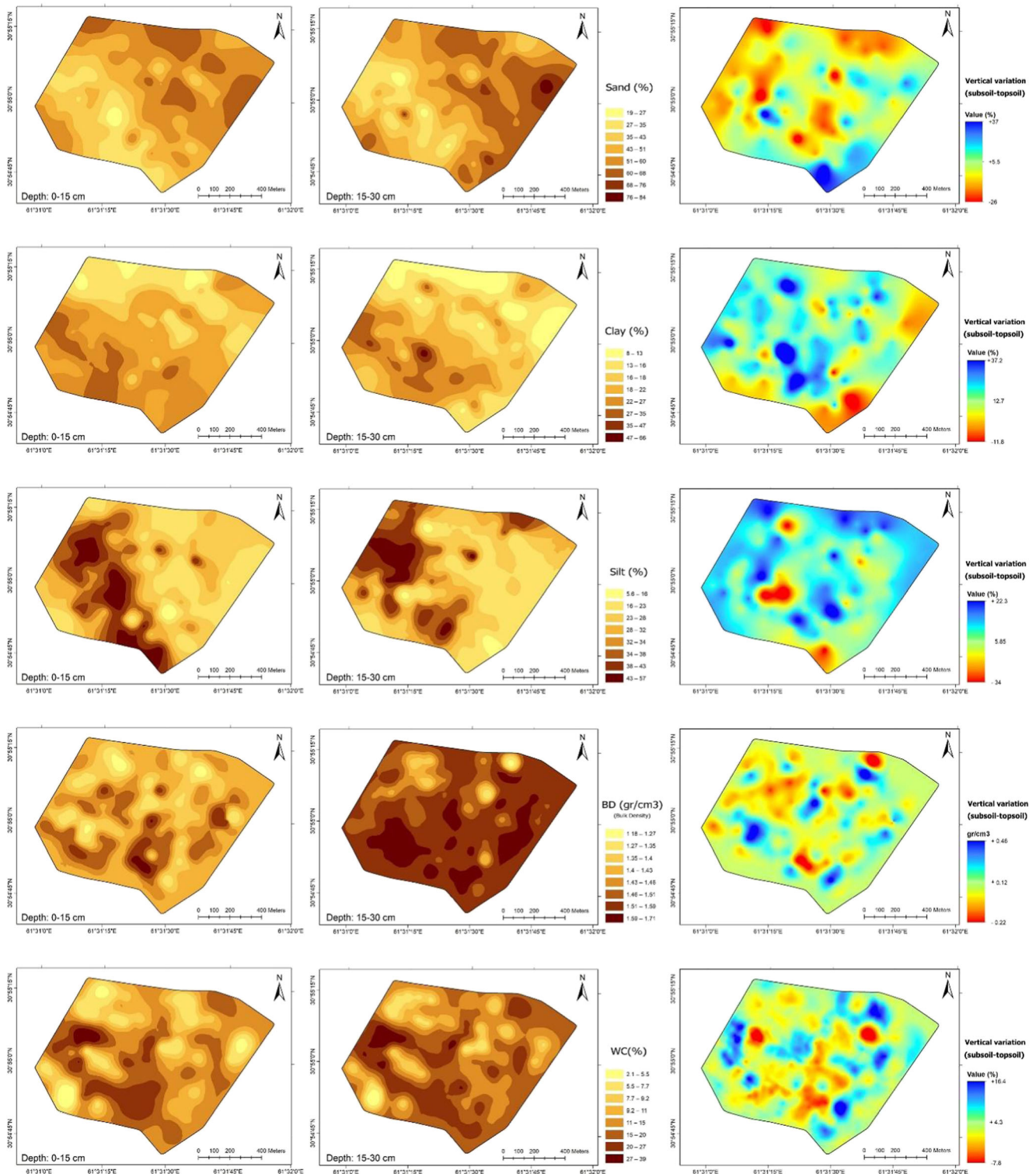

Fig. 2 Mapping soil properties using the best interpolation method for depth intervals 0–15 cm and 15–30 cm. Also shown in the right is the amount of variation between two layers
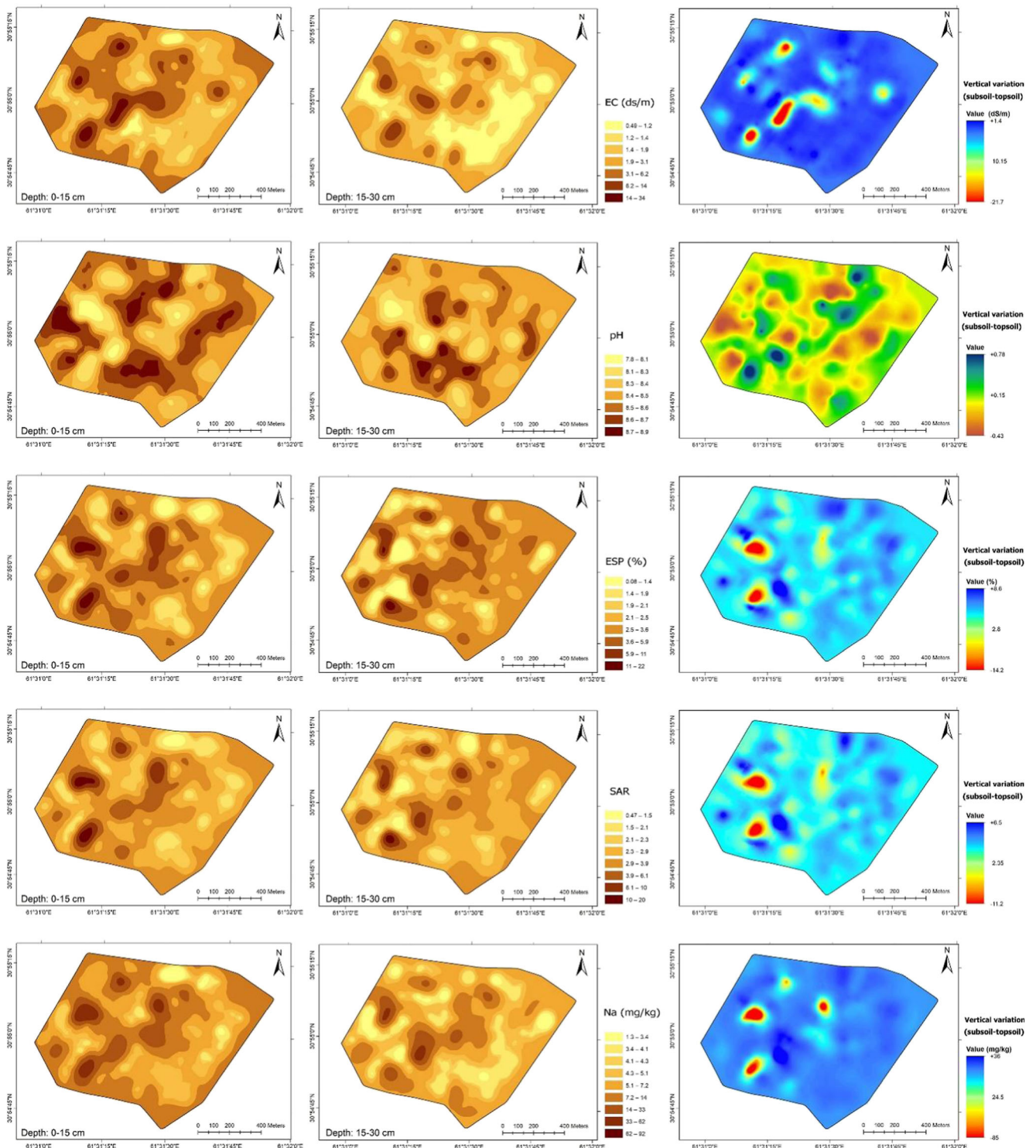
Fig. 2 continued.

texture. Due to the use of saline irrigation water of local wells in the time of water shortage and a high evaporation rate, salt has been accumulation mostly in cultivated areas while less EC is seen in non-cultivated areas, e.g., in the northwest of the field. The maps of pH in Fig. 2 show that acidity has a similar spatial pattern over the study region for both depths. Majority

of the region has a pH value of greater than 8, indicating an alkaline condition over the study field. Moreover, the map of difference between two depths shows that pH increased with depth in some regions and decreased in other parts. Prolong drought and frequent use of saline water for irrigation resulted in a high amount of SAR for two layers over the study area
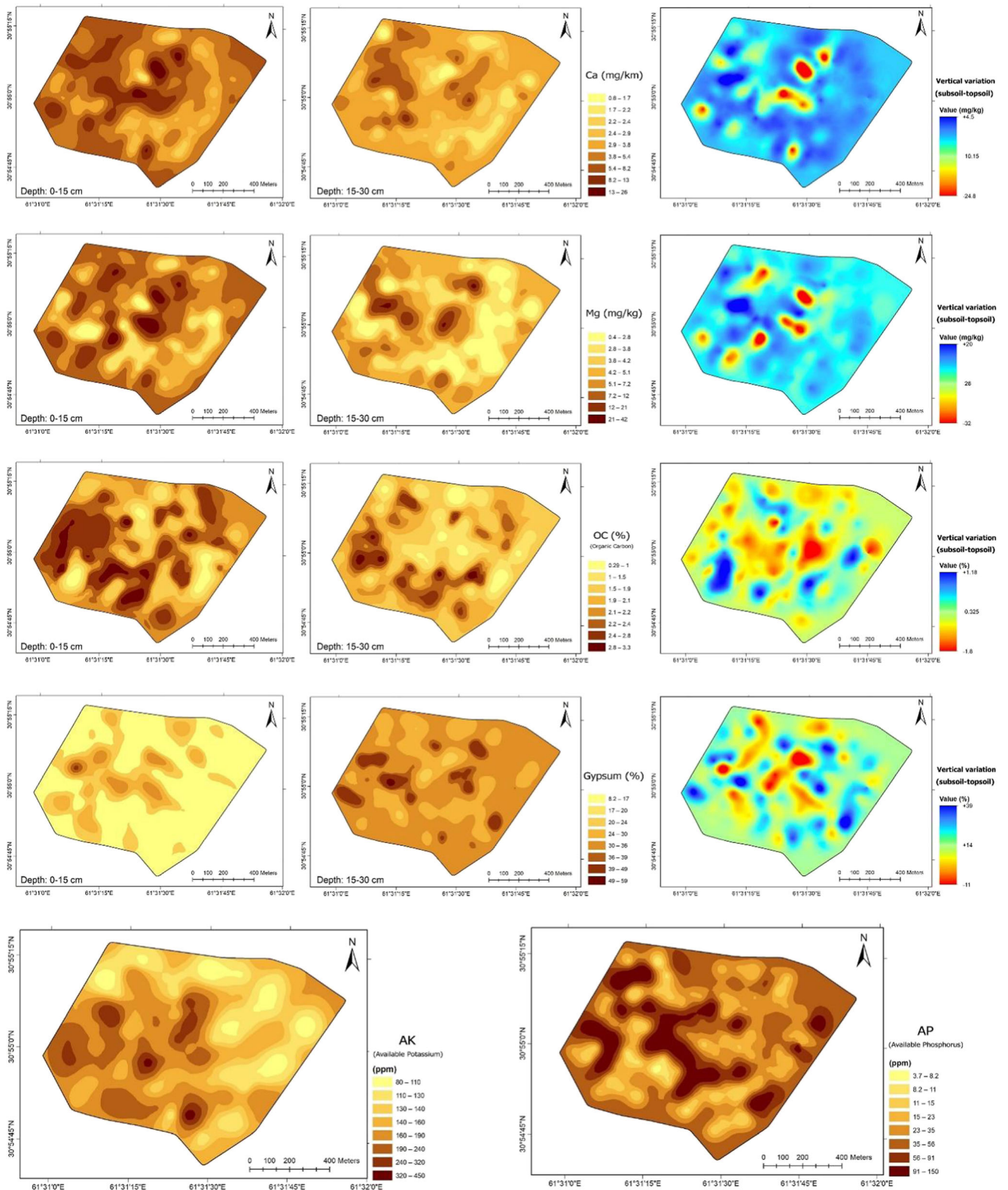
Fig. 2 continued.

(Fig. 2). The amount of SAR increased toward the center and southern regions; herein, soil contains more clay content, causing more limitation (e.g., lowers soil infiltration rate) for

agricultural production. The spatial distribution maps of gypsum show that the higher amount of gypsum is seen in subsoil than topsoil since low soluble gypsum is deposited in deeper

layers following basin irrigation traditionally used for irrigation purposes over the study region. The map of topsoil OC shows that almost two third of study area has an OC content of 2 to 3%. However, for 15–30-cm depth, OC in most parts is below 2%, which is the critical limit for organic carbon in most agricultural calcareous soils. The major driving factors for low concentration of OC over study area could be long-term cultivation practices (Safadoust et al. 2016a), wind erosion (Yan et al. 2005), and low water content and high soil temperature (Callesen et al. 2003). As mentioned by Lal (1990) and Afrasiab and Delbari (2013), low amount of soil water content due to low rainfall and irrigation along with strong wind may cause soil degradation and desertification through wind erosion. Soil erosion removes the fertile surface soil, affects OC content and soil biological activities, and limits plant growth (Yan et al. 2005; Tanner et al. 2016). Li et al. (2008) stated that *wind erosion might affect* the spatial heterogeneity of *soil* nutrients such as OC. Low amount of OC is typical in soils of Aridisols and Entisols orders (Eswaran and Reich 2005; Guo et al. 2006). However, to reduce wind erosion and in turn soil organic carbon losses, proper soil conservation practices and soil fixation should be adapted (Salem 1989). Implementation of best management practices (BMPs) such as conservation tillage, organic cropping, and irrigation water management can enhance soil OC concentration (Sharma et al. 2011) and therefore improve soil quality over the study region.

To better realize the vertical variation of selected soil properties over the whole field, the percent of study area where the amount of each variable is increased in subsoil when compared to topsoil is also calculated and the results are presented in Table 6. As seen, soil physical properties including Silt,

Table 6 The percent of study area where each soil property is increased in subsoil relative to topsoil

Variable	Percent area (%)
Clay (%)	21.6
Silt (%)	64.6
Sand (%)	38.4
BD (gr/cm^3)	97.9
WC (%)	92.6
EC (dSm)	2.2
ESP	28.9
SAR	22.7
pH	31.5
Na (mg/kg)	11.5
Ca (mg/kg)	4.1
Mg (mg/kg)	8.8
Gypsum (%)	99.5
OC (%)	11

BD, and WC increased in subsoil in more than 60% of the study area, while most soil chemical properties, i.e., EC, ESP, SAR, pH, Na, Ca, Mg, and OC, decreased in subsoil in more than 70% of the study area. Clay and Sand increased in subsoil in about 22% and 38% of the study area, respectively. The high amounts of soil chemical properties in topsoil are corresponding to a high ratio of evaporation to precipitation which causes the upward movement of dissolved nutrients in the soil profile (Yu et al. 2014). On the other hand, a relatively lighter soil texture in deeper layer and infrequent basin irrigation cause nutrients leaching through deep percolating water (Lehmann and Schroth 2003).

Figure 2 also shows the spatial distribution of AP and AK. As expected from auto-correlation analysis (Table 3), spatial distribution map of AP shows little spatial continuity (small and high values of AP occur near to each other). In contrast, the estimation map of AK shows a good spatial continuity of AK with an increase along the northeast toward the southwest of the study area as soil texture gets heavier. Almost half the study region (north, northwest, and east) has an AK less than 170 ppm, which is a critical limit for agricultural production (Karlen et al. 1994). The high and low amounts of AP and AK revealed that their spatial pattern might be also influenced by anthropogenic causes such as fertilization.

Conclusion

The main goal of this this study is to predict the spatial distribution of topsoil (0–15 cm) and subsoil (15–30 cm) physical and quality parameters in an agriculture field in an arid and semi-arid region. The study is also aimed to explore the inter-relationship between soil properties and their vertical variation in two successive layers of a salt-affected soil. Statistical analysis showed that soil chemical properties have a moderate to high coefficient of variation while physical properties and pH have a low to moderate coefficient of variation over the study area. Pearson correlation matrix indicated a significant correlation among soil attributes especially for the topsoil. All soil properties showed a degree of spatial correlation from moderate to strong with a small to large spatial correlation distance. Physical soil properties, i.e., the percentage of sand, silt, and clay, are correlated fairly well in space with a large correlation distance. However, most of soil chemical properties such as pH, ESP, SAR, EC, and AP showed small correlation distance, which reflects the influence of agriculture activities and land use pattern on the spatial autocorrelation of soil chemical properties. According to cross-validation results, for most soil properties, either the LOK or IDW method provided the least interpolation error. The maps of soil texture fractions spatial distribution showed that soil texture is coarser near the riverbank in north and northeast of study area. However, in most areas, the amount of clay decreased in

15–30 cm compared to 0–15 cm. The comparison of soil property spatial distributions for two layers showed an accumulation of soil chemical properties, e.g., Ca, Mg, and Na, at topsoil mostly due to low precipitation and high evaporation rates over the study region. The maps of EC and pH clearly show that soils in the study region are mostly saline and alkaline. Moreover, OC concentration was shown to be almost at the minimum level for agricultural production. BMPs such as conservation tillage, agricultural water management, organic farming, land restoration, and land use change are needed to increase OC concentration, balance water, and temperature regime in soil and improve soil quality for a better plant growth. The generated maps of soil physical attributes and soil nutrients can help farmers and decision makers for an optimum water and nutrient management. For example, large contents of AP and AK were observed in some parts of study area mainly due to human activities. Future nutrient and fertilizer applications should include a site-specific condition to not only reduce the cost of input management but also to prevent any environmental hazard.

References

Abegaz A, Adugna A (2015) Effects of soil depth on the dynamics of selected soil properties among the highlands resources of northeast Wollega, Ethiopia: are these sign of degradation? Solid Earth Discussions 7(3)

Adhikari G, Bhattacharyya KG (2015) Correlation of soil organic carbon and nutrients (NPK) to soil mineralogy, texture, aggregation, and land use pattern. Environ Monit Assess 187:735

Afrasiab P, Delbari M (2013) Assessing the risk of soil vulnerability to wind erosion through conditional simulation of soil water content in Sistan plain, Iran. Environ Earth Sci 70:2895–2905

Amini M, Afyuni M, Khademi H, Abbaspour KC, Schulin R (2005) Mapping risk of cadmium and lead contamination to human health in soils of Central Iran. Sci Total Environ 347:64–77

Ayoubi SH, Mohammad Zamani S, Khormali F (2012) Spatial variability of some soil properties for site specific farming in northern Iran. Intl J Plant Prod 1(2):225–236

Basso B, Ritchie JT (2015) Simulating crop growth and biogeochemical fluxes in response to land management using the SALUS model. In: The ecology of agricultural landscapes: long-term research on the path to sustainability. Oxford University press, New York, NY USA, pp 252–274

Basso B, Bertocco M, Sartori L, Martin EC (2007) Analyzing the effects of climate variability on spatial pattern of yield in a maize-wheat-soybean rotation. Eur J Agron 26:82–91

Bhatti AU, Bakhsh A, Afzal M, Gurmani AH (1999) Spatial variability of soil properties and wheat yields in an irrigated field. Commun Soil Sci Plant Anal 30:1279–1290

Blake GR, Hartge KH (1986) Bulk density. In: Klute, a., Ed., methods of soil analysis, part 1-physical and mineralogical methods, 2nd ed. agronomy monograph 9, am Soc Agron-soil Sci Soc am, Madison

Blumfield TJ, Zhi-Hong XU, Prasolova NV (2007) Sampling size required for determining soil carbon and nitrogen properties at early establishment of second rotation hoop pine plantations in subtropical Australia. Pedosphere 17:706–711

Boekhold AE, Van der Zee SE (1992) Significance of soil chemical heterogeneity for spatial behavior of cadmium of cadmium in field soils. Soil Sci Soc Am J 56:747–754

Bogunovic I, Trevisani S, Seput M, Juzbasic D, Durdevic B (2017) Short-range and regional spatial variability of soil chemical properties in an agro-ecosystem in eastern Croatia. Catena 154:50–62

Bouma J, Stoorvogel J, van Alphen BJ, Booltink HWG (1999) Pedology, precision agriculture, and the changing paradigm of agricultural research. Soil Sci Soc Am J 63(6):1763–1768

Box GE, Cox DR (1964) An analysis of transformations. J Royal Stat Soc Series B (Methodological) 26:211–252

Brouder SM, Hofmann BS, Morris DK (2005) Mapping Soil pH. Soil Sci Soc Am J 69:427–442

Brus DJ, Heuvelink GBM (2007) Optimization of sample patterns for universal kriging of environmental variables. Geoderma 138:86–95

Burgess TM, Webster R (1980) Optimal interpolation and isar1thmic mapping of soil properties. Eur J Soil Sci 31:315–331

Callesen I, Liski J, Raulund-Rasmussen K, Olsson MT, Tau-Strand L, Vesterdal L, Westman CJ (2003) Soil carbon stores in Nordic well-drained forest soils—relationships with climate and texture class. Glob Chang Biol 9:358–370

Cambardella CA, Moorman TB, Novak JM, Parkin TB, Turco RF, Konopka AE (1994) Field scale variability of soil properties in Central Iowa soils. Soil Sci Soc Am J 58:1501–1511

Cemek B, Guler M, Kilic K, Demir Y, Arslan H (2007) Assessment of spatial variability in soil properties as related to soil salinity and alkalinity in Bafra plain in northern Turkey. Environ Monit Assess 124:223–234

Chung CK, Chong SK, Varsa EC (1995) Sampling strategies for fertility on a stoy silt loam soil. Commun Soil Sci Plant Anal 26(5-6):741–763

Clark I (1979) Practical geostatistics. Applied Science Publishers, London

Delbari M, Afrasiab P, Loiskandl W (2009) Using sequential Gaussian simulation to assess the field-scale spatial uncertainty of soil water content. Catena 79:163–169

Delbari M, Loiskandl W, Afrasiab P (2010) Uncertainty assessment of soil organic carbon content spatial distribution using geostatistical stochastic simulation. Soil Res 48:27–35

Delbari M, Afrasiab P, Loiskandl W (2011) Geostatistical analysis of soil texture fractions on the field scale. Soil Water Res 6:173–189

Eswaran H, Reich PF (2005) World soil map. In: Hillel D, Hatfield JL (eds) Encyclopedia of soils in the environment (Vol. 3). Elsevier, Amsterdam

Evrendilek F, Celik I, Kilic S (2004) Changes in soil organic carbon and other physical soil properties along adjacent Mediterranean forest, grassland, and cropland ecosystems in Turkey. J Arid Environ 59:743–752

Fu W, Tunney H, Zhang C (2010) Spatial variation of soil nutrients in a dairy farm and its implications for site-specific fertilizer application. Soil Tillage Res 106:185–193

Gallardo A, Paramá R (2007) Spatial variability of soil elements in two plant communities of NW Spain. Geoderma 139:199–208

Gee GW, Bauder JW (1986) Particle-size analysis, hydrometer method. In a Klute et al. (eds.) methods of soil analysis, part I.3rd ed., am Soc Agron, Madison

Geypens M, Vanongeval L, Vogels N, Meykens J (1999) Spatial variability of agricultural soil fertility parameters in a gleyic podzol of Belgium. Precis Agric 1:319–326

Gomez JA, Vanderlinden K, Nearing MA (2005) Spatial variability of surface roughness and hydraulic conductivity after disk tillage: implications for runoff variability. J Hydrol 311:143–156

Goovaerts P (1997) Geostatistics for natural resources evaluation. Oxford University Press

Goovaerts P (1998) Geostatistical tools for characterizing the spatial variability of microbiological and physico-chemical soil properties. Biol Fertil Soils 27:315–334

Goovaerts P (1999) Geostatistics in soil science: state of the art and perspectives. Geoderma 89:1–45

Goovaerts P, AvRuskin G, Meliker J, Slotnick M, Jacquez G, Nriagu J (2005) Geostatistical modeling of the spatial variability of arsenic in groundwater of Southeast Michigan. Water Resour Res 41:1–19

Gotway CA, Ferguson RB, Hergert GW, Peterson TA (1996) Comparison of kriging and inverse-distance methods for mapping soil parameters. Soil Sci Soc Am J 60:1237–1247

Goulard M, Voltz M (1992) Linear coregionalization model: tools for estimation and choice of cross-variogram matrix. Math Geol 24(3):269–286

Guo Y, Amundson R, Gong P, Yu Q (2006) Quantity and spatial variability of soil carbon in the conterminous United States. Soil Sci Soc Am J 70(2):590–600

Haan CT (2002) Statistical methods in hydrology. The Iowa State University Press

Hirzel A, Guisan A (2002) Which is the optimal sampling strategy for habitat suitability modelling. Ecol Model 157:331–341

Huang X, Skidmore EL, Tibke G (2001) Spatial variability of soil properties along a transect of CRP and continuously cropped land. Sustaining the Global Farm: 24–29

Iqbal J, Thomasson JA, Jenkins JN, Owens PR, Whisler FD (2005) Spatial variability analysis of soil physical properties of alluvial soils. Soil Sci Soc Am J 69:1338–1350

Isaaks EH, Srivastava RM (1989) Applied Geostatistics: Oxford University press, New York

Jawad IT, Taha MR, Majeed ZH, Khan TA (2014) Soil stabilization using lime: advantages, disadvantages and proposing a potential alternative. Res J Appl Sci Eng Technol 8:510–520

Journel AG, Huijbregts CJ (1978) Mining geostatistics. Academic press, London

Karlen DL, Wollenhaupt NC, Erbach DC, Berry EC, Swan JB, Eash NS, Jordahl JL (1994) Long-term tillage effects on soil quality. Soil Tillage Res 32:313–327

Kerry R, Oliver MA (2004) Average variograms to guide soil sampling. Intl J Appl Earth Obs 5(4):307–325

Kravchenko A, Bullock DG (1999) A comparative study of interpolation methods for mapping soil properties. Agron J 91:393–400

Lal R (1990) Soil erosion and land degradation: the global risks. In advances in soil science. Springer, New York

Lal R (2015) Restoring soil quality to mitigate soil degradation. Sustainability 7:5875–5895

Laslett GM, McBratney AB, Pahl P, Hutchinson MF (1987) Comparison of several spatial prediction methods for soil pH. Eur J Soil Sci 38: 325–341

Lehmann J, Schroth G (2003) Nutrient leaching. Trees, crops, and soil fertility: concepts and research methods. Wallingford, UK: CAB international: 151-166

Li J, Okin GS, Alvarez L, Epstein H (2008) Effects of wind erosion on the spatial heterogeneity of soil nutrients in two desert grassland communities. Biogeochemistry 88:73–88

Ma Y, Minasny B, Wu C (2017) Mapping key soil properties to support agricultural production in eastern China. Geoderma Reg 10:144–153

MacCarthy DS, Agyare WA, Vlek PLG, Adiku SGK (2013) Spatial variability of some soil chemical and physical properties of an agricultural landscape. West Afr J Appl Ecol 21(2013):47–61

McBratney AB, Webster R (1983) How many observations are needed for regional estimation of soil properties? Soil Sci 135:177–183

McGrath D, Zhang C, Carton OT (2004) Geostatistical analyses and hazard assessment on soil lead in Silvermines area, Ireland. Environ Pollut 127:239–248

McGrath D, Zhang C (2003) Spatial distribution of soil organic carbon concentrations in grassland of Ireland. Appl Geochem 18(10):1629–1639

Mirakzehi K, Pahlavan-Rad MR, Shahriari A, Bameri A (2018) Digital soil mapping of deltaic soils: a case of study from Hirmand (Helmand) river delta. Geoderma 313:233–240

Morgan RPC (2005) Soil erosion and conservation. Blackwell Science Ltd., Oxford, p 304

Mulla DJ (1991) Using geostatistics and GIS to manage spatial patterns in soil fertility. In: Kranzler G (ed) Automated Agriculture for the 21st Century. Am. Soc. Ag. Eng, St. Joseph, pp 336–345

Nichols JD (1984) Relation of organic carbon to soil properties and climate in the southern Great Plains 1. Soil Sci Soc Am J 48:1382–1384

Norušis MJ (2002) SPSS 11.0 guide to data analysis. Prentice Hall, Upper Saddle River

USDA-NRCS (1996) Soil survey laboratory methods manual. Soil survey investigations report 42, Version 3.0. US Department of Agriculture, Natural Resources Conservation Service, Washington, DC

Olsen SR, Cole CV, Watanabe FS, Dean LA (1954) Estimation of available phosphorous in soil by extraction with sodium bicarbonate. USDA. Cire. 939. U. S. Gov. print. Office, Washington D.C.

Ontl TA, Schulte LA (2012) Soil carbon storage. Nat Educ Knowledge 3: 35

Reeves DW (1997) The role of soil organic matter in maintaining soil quality in continuous cropping systems. Soil Tillage Res 43:131–167

Rhoades JD (1996) Salinity: electrical conductivity and total dissolved solids. Methods of soil analysis part 3-chemical methods, am Soc Agron, Medison

Robertson GP (2008) GS+: Geostatistics for the environmental sciences. Gamma Design Software, Plainwell

Robinson TP, Metternicht G (2006) Testing the performance of spatial interpolation techniques for mapping soil properties. Comput Electron Agric 50:97–108

Rosemary F, Indraratne SP, Weerasooriya R, Mishra U (2017) Exploring the spatial variability of soil properties in an Alfisol soil catena. Catena 150:53–61

Safadoust A, Doaei N, Mahboubi AA, Mosaddeghi MR, Gharabaghi B, Voroney P, Ahrens B (2016a) Long-term cultivation and landscape position effects on aggregate size and organic carbon fractionation on surface soil properties in semi-arid region of Iran. Arid Land Res Manag 30:345–361

Safadoust A, Amiri Khaboushan E, Mahboubi AA, Gharabaghi B, Mosaddeghi MR, Ahrens B, Hassanpour Y (2016b) Comparison of three models describing bromide transport affected by different soil structure types. Arch Agron Soil Sci 62:674–687

Sakin E (2012a) Organic carbon organic matter and bulk density relationships in arid-semi arid soils in Southeast Anatolia region. Afr J Biotechnol 11:1373–1377

Sakin E (2012b) Relationships between of carbon, nitrogen stocks and texture of the Harran plain soils in southeastern Turkey. Bulgarian J Agri Sci 18:626–634

Salem BB (1989) Arid zone forestry: a guide for field technicians (no. 20). Food and agriculture organization (FAO)

Schepers JS, Schlemmer MR, Ferguson RB (2000) Site-specific considerations for managing phosphorus. J Environ Qual 29:125–130

Schollenberger CJ, Simon RH (1945) Determination of exchange capacity and exchangeable bases in soil-ammonium acetate method. Soil Sci 59:13–24

Sharma P, Singh G, Singh RP (2011) Conservation tillage, optimal water and organic nutrient supply enhance soil microbial activities during wheat (Triticum aestivum L.) cultivation. Braz J Microbiol 42:531–542

Shukla MK, Slater BK, Lal R, Cepuder P (2004) Spatial variability of soil properties and potential management classification of a chernozemic field in lower Austria. Soil Sci 169(12):852–860

Soil Survey Division Staff (2017) Soil survey manual. 4th In USDA Handbook 18, USDA-Nat. Resour. Conserv. Serv., Ed Ditzler C, Scheffe K, Monger HC, Government Printing Office, Washington DC

Stang C, Gharabaghi B, Rudra R, Golmohammadi G, Mahboubi AA, Ahmed SI (2016) Conservation management practices: success story of the hog creek and sturgeon river watersheds, Ontario, Canada. J Soil and Water Conserv 71:237–248

Sun B, Zhou S, Zhao Q (2003) Evaluation of spatial and temporal changes of soil quality based on geostatistical analysis in the hill region of subtropical China. Geoderma 115:85–99

Tabor JA, Warrick AW, Myers DE, Pennington DA (1985) Spatial variability of nitrate in irrigated cotton: II. soil nitrate and correlated variables 1. Soil Sci Soc Am J 49(2):390–394

Tanner S, Katra I, Haim A, Zaady E (2016) Short-term soil loss by eolian erosion in response to different rain-fed agricultural practices. Soil Tillage Res 155:149–156

Thayer WC, Griffith DA, Goodrum PE, Diamond GL, Hassett JM (2003) Application of geostatistics to risk assessment. Risk Anal 23:945–960

Thomas GW (1996) Soil pH and soil activity. In: Sparks DL et al (eds) Method of soil analysis, part 3. Am Soc Agron, Medison

Trangmar BB, Yost RS, Uehara G (1985) Application of geostatistics to spatial studies of soil properties. Adv Agron 38:45–94

US Salinity Laboratory Staff (1954) Diagnosis and improvement of saline and alkali soils. USDA Handbook 60. US Government Printing Office, Washington D C

Vachaud G, Chen T (2002) Sensitivity of computed values of water balance and nitrate leaching to within soil class variability of transport parameters. J Hydrol 264:87–100

Van Alphen JG, de los Ríos Romero F (1971) Gypsiferous soils: notes on their characteristics and management (no. 12). ILRI

Vasu D, Singh SK, Sahu N, Tiwary P, Chandran P, Duraisami VP, Kalaiselvi B (2017) Assessment of spatial variability of soil properties using geospatial techniques for farm level nutrient management. Soil Tillage Res 169:25–34

Walter C, McBratney AB, Douaoui A, Minasny B (2001) Spatial prediction of topsoil salinity in the Chelif Valley, Algeria, using local ordinary kriging with local variograms versus whole-area variogram. Soil Res 39(2):259–272

Wang G, Gertner G, Howard H, Anderson A (2008) Optimal spatial resolution for collection of ground data and multi-sensor image mapping of a soil erosion cover factor. J Environ Manag 88:1088–1098

Warrick AW (1998) Spatial variability. In: Hillel D (ed) Environmental soil physics. Academic Press, San Diego

Wollenhaupt NC, Wolkowski RP, Clayton MK (1994) Mapping soil test phosphorus and potassium for variable-rate fertilizer application. J Prod Agri 7:441–448

Yan H, Wang S, Wang C, Zhang G, Patel N (2005) Losses of soil organic carbon under wind erosion in China. Glob Chang Biol 11:828–840

Yu J, Li Y, Han G, Zhou D, Fu Y, Guan B, Wang G, Ning K, Wu H, Wang J (2014) The spatial distribution characteristics of soil salinity in coastal zone of the Yellow River Delta. Environ Earth Sci 72:589–599

Zhang C (2006) Using multivariate analyses and GIS to identify pollutants and their spatial patterns in urban soils in Galway, Ireland. Environ Pollut 142(3):501–511

Zhang WT, Hong-Qi WU, Hai-Bin GU, Guang-Long FENG, Ze WANG, Sheng JD (2014) Variability of soil salinity at multiple spatio-temporal scales and the related driving factors in the oasis areas of Xinjiang, China. Pedosphere 24:753–762